Available online at www.sciencedirect.com
ScienceDirect
Polymer 48 (2007) 5950–5959
polymer
www.elsevier.com/locate/polymer

Studies on preparation and properties of PAA/gelatin core-shell nanoparticles via template polymerization

Yansong Wang, Youwei Zhang*, Chengxun Wu, Jiongxin Zhao

State Key Laboratory for Modification of Chemical Fibers and Polymer Materials, Institute of Chemical Fibers, College of Material Science and Engineering, Donghua University, Shanghai 201620, PR China

Received 28 April 2007; received in revised form 7 August 2007; accepted 8 August 2007
Available online 14 August 2007

Abstract

Taking advantage of the simultaneous polymerization and self-assembly between the components during the template polymerization, narrowly distributed nanoparticles with core-shell structure were prepared at high concentrations via polymerizing acrylic acid (AA) in aqueous solution of template gelatin. The influences of various polymerization parameters such as medium pH, concentration, and ratio of AA/gelatin were systematically investigated, which indicates that the size and structure of the nanoparticles can be adjusted by changing the reaction conditions. The nanoparticles are stimuli-responsive: the nanoparticles' size increases when increasing or decreasing pH value from about 2.8 while it first decreases slightly and then increases monotonically as salt concentration increases. Also, the nanoparticles exhibit a stronger salt-resistance as compared with those prepared by dropping method. The structure of the nanoparticles was further locked by selectively crosslinking gelatin with glutaraldehyde. The size and swelling capacity of the nanoparticles decrease with the increase of crosslinking degree.

Keywords: Gelatin; Stimuli-response; Nanoparticles

1. Introduction

Polymeric nanoparticles with hydrophilic outer shell and hydrophobic inner core have attracted great interest because of their potential applications in various fields [1–5]. Specifically, the nanoparticles in a size range of 10–200 nm would be an ideal candidate as drug carriers for their ''passive'' targeting [6–8]. Self-assembly was an efficient approach to fabricate nanoparticles from amphiphilic copolymers. For example, Wooley obtained stable core-shell nanoparticles via self-assembly of di-block copolymers and succedent crosslinking of the 'shell' part of the micelles [9]. Armes prepared stable shell-crosslinked micelles at high concentrations (100 mg/mL) via crosslinking the shell of 'core-shell-corna' micelles from tri-block copolymers [10]. Chen obtained core-crosslinked micelles at high solids via selectively crosslinking one block of di-block copolymers in their co-solvent [11]. However, their need to synthesizing block copolymers limits their practical application.

Nowadays, bio-macromolecules and their derivatives, due to their unique physicochemical properties, are increasingly used to prepare various materials including nanoparticles, especially those for biomedical purposes. For example, core-shell nanoparticles were fabricated from chitosan and poly(acrylic acid) (PAA) [12]; hollow nanoparticles were synthesized via polymerizing AA in the presence of chitosan [13]; stabilized pH-responsive nanoparticles were prepared from dextran and AA monomers [14].

Aimed at improving the practicability of polymeric nanoparticles with good biocompatibility for biomedical use, we previously reported a convenient way to prepare biocompatible core-shell polymeric nanoparticles at high concentrations via template polymerization in a complete aqueous medium using gelatin and AA as a reaction system [15]. We found that PAA/gelatin nanoparticles with cores of insoluble gelatin–PAA interpolymer complexes and shells of soluble gelatin

* Corresponding author. Tel.: +86 21 67792889; fax: +86 21 67792855.
E-mail address: zhyw@dhu.edu.cn (Y. Zhang).

0032-3861/$ - see front matter © 2007 Elsevier Ltd. All rights reserved.
doi:10.1016/j.polymer.2007.08.019

were produced due to the specific interactions between gelatin and PAA produced *in situ*. Because of the simultaneous polymerization and self-assembly in the template polymerization, which slows down the self-assembly between the components, the nanoparticles can be prepared at high concentrations. However, the parameter-dependence of the reaction and stimuli-response of the nanoparticles were not involved. In this article, we report the results of a detailed study on the reaction, including the effects of reaction parameters such as pH of medium, concentration, ratio of AA/gelatin on the reaction process and nanoparticles' structure, and the influences of crosslinking, pH, and salt on the size and stability of the nanoparticles.

2. Experimental section

2.1. Materials

Gelatin (gelatin B) from Nanxiang Chemical Co. Ltd was of chemical grade. Acrylic acid (AA) from Shanghai Chemical Co. Ltd. was purified by vacuum distillation. Ammonium persulfate (APS) from Shanghai Qianjin Chemical Plant and *N*,*N*,*N*′,*N*′-tetramethylethylene diamine (TEMED) from Merck Co. Ltd. were of analytical grade. Glutaraldehyde (GA) aqueous solution (25%) was purchased from Shanghai Chemical Co. Ltd.

2.2. Preparation of PAA/gelatin nanoparticles via dropping method

First, a PAA aqueous solution of 4 mg/mL and a gelatin aqueous solution of 2 mg/mL were prepared. Then, pH of the two solutions was adjusted to about 2.8. PAA/gelatin nanoparticles were prepared by adding 3 mL of PAA solution dropwise slowly into 3 mL of gelatin solution under stirring.

2.3. Preparation of PAA/gelatin nanoparticles via template polymerization

A typical process was as follows: gelatin (0.6 g) was first dissolved in 60 mL of aqueous solution (denoted as medium solution) of pH 2.5, followed by filtration to remove insoluble impurities. Next, AA (1.2 mL) was added to the purified gelatin solution under stirring in a nitrogen atmosphere. After temperature was raised to 40 °C, initiator APS and accelerator TEMED were added to initiate the polymerization. The reaction was allowed to proceed for 3 h, and residual monomers were removed by dialyzing against HCl solution of an equal pH for 48 h using a dialysis membrane bag (14 kDa cut-off).

2.4. Crosslinking of PAA/gelatin nanoparticles

A determined amount of GA was added to the nanoparticles' dispersion under stirring at 40 °C, the reaction occurred for 2 h and was terminated by dialyzing against HCl solution with the same pH.

2.5. Measurements

The molecular weight of PAA in the nanoparticles was evaluated by viscosimetry. First dissolve the nanoparticles by adjusting pH of the dispersion to around 10, and then precipitate the gelatin by adjusting pH value to around its isoelectric point. After that, the dispersion was separated by centrifugation and the supernatant was used for viscosity measurements. The PAA concentration of the supernatant was determined by ultraviolet spectrometry using the absorbance at 202 nm. As the molecular weight of PAA in the nanoparticles is very low, the intrinsic viscosity ($[\eta]$) of PAA solution cannot be determined by dilution method, and thus was estimated from the relative viscosity (η_r) of a dilute solution of PAA in 2 mol/L NaOH aqueous solution ($C = 0.16$ mg/mL). In addition, three samples (sodium salt of PAA, Aldrich) with known molecular weights ($M_W = 5100$, 8000, 15,000, measured by GPC) were used to determine the values of parameter K and α in Mark–Houwink equation.

FTIR spectra were obtained on a Nicolet Magna 550 spectrometer as KBr pellets. Hydrodynamic diameter, size distribution and ζ potential of the nanoparticles were determined using Malvern DTS1060. The results were averaged on three times of measurements. Fluorescence spectra were measured using a JASCO FP-6500 spectrometer. Using pyrene probe, emission spectra were obtained by exciting at 334 nm at a pyrene concentration of 2×10^{-7} mol/L. Transmission electron microscopy (TEM) observations were performed on a Philips CM120 electron microscope at an accelerating voltage of 80 kV. The samples were prepared by placing one drop of nanoparticles' dispersion on copper grids and allowing them to dry in the air for 24 h. Atomic force microscopy (AFM) observations were conducted with a Nanoscope IV (Digital Instruments) atomic force microscope in tapping mode. The sample preparation for AFM observations was similar to that for TEM, except that freshly-cleaved mica substrate was used.

3. Results and discussion

3.1. Parameters' effects on the polymerization process

3.1.1. Medium pH effects

As revealed in our previous papers [15], because of the self-assembly between gelatin and PAA co-driven by hydrogen bonding and electrostatic interactions, PAA/gelatin nanoparticles, with cores of insoluble gelatin–PAA interpolymer complexes and shells of soluble gelatin, formed spontaneously during the template polymerization. The interactions are closely related to the ionization of the components and thus pH of the medium. In order to understand the relation between the property of the specific interactions and the structure of the nanoparticles, we examined the polymerizations in aqueous media with different pH values. Gelatin tends to degrade in strong acid media; meanwhile, nanoparticles formed *in situ* tend to aggregate and form micro-precipitates as pH is close to the isoelectric point (IP) of gelatin shell. It was found that the polymerization occurred smoothly only in a narrow pH

range of 1.9–2.8, and pH diversity was exhibited among the various solutions including medium solution, gelatin solution, the initial reaction solution and the final reaction solution (i.e. nanoparticles' solution). As revealed by Table 1, the pH discrepancy (1.9–2.8) among the initial reaction solution became very small as compared with the medium solution (1.7–9.0), which was mainly caused by the protonation of amino group of gelatin and the ionization of carboxy of AA and gelatin. In addition, pH of the reaction solution increased slightly after polymerization, which may result from the difference in pK_a of AA (4.25) [13] and PAA (4.75) [16].

We also used DTS to trace all the polymerizations and found that the changes of ζ potential and size of the reaction solutions with the polymerization time were similar. Typical curves of $\langle D_h \rangle$ vs. time and ζ potential vs. time for polymerization adopting a medium solution of pH 3.0 are displayed in Fig. 1, as an example. Accompanied by a continuous decrease in the hydrodynamic diameter of the reaction solution, ζ potential decreased in the first 0.5 h and then kept almost constant with the time.

In the initial reaction solution, soluble complexes of gelatin and AA with a loose structure were produced due to the interactions between them. Upon polymerization of AA, PAA produced *in situ* self-assembled with gelatin to form assemblies with hydrophobic PAA–gelatin complex cores and hydrophilic gelatin shells (i.e. PAA/gelatin nanoparticles). Since the interactions between the components were enhanced as AA small molecules were converted to PAA, the structure of PAA–gelatin complexes was compact as compared with gelatin–AA complexes and hence resulting in PAA/gelatin nanoparticles of smaller size and ζ potential. As the polymerization continued, more and more PAA/gelatin nanoparticles were produced at the cost of soluble gelatin–AA complexes. As a result, the $\langle D_h \rangle$ of the reaction solution decreased slowly while ζ potential remained almost constant.

As indicated in Fig. 2, the nanoparticles' size decreased with pH of medium solution in a pH range of 1.7–3.0 while increased on the contrary when further increasing the pH. As the pH increased, due to the ionization of PAA, the electrostatic interactions between the components enhanced at the cost of the hydrogen bonding interactions. Meanwhile, as indicated by the ζ potential of the nanoparticles, the repulsive interactions among gelatin chains of the nanoparticles' shell also decreased with the pH except for the case of medium solution of pH 1.7. Both the changes favored the formation of assemblies with more compact structure, and hence, the

Table 1
pH data of medium solution, gelatin solution and reaction solutions[a]

Medium solution[b]	9.0	5.5	3.0	2.5	2.0	1.7
Gelatin solution	7.8	5.8	4.3	3.8	3.2	2.0
Initial reaction solution	2.8	2.7	2.6	2.5	2.2	1.9
Nanoparticles' solution	3.1	3.0	2.9	2.8	2.5	2.1

[a] Concentration of gelatin and AA are 10 mg/mL and 20 mg/mL, respectively.
[b] pH of medium solution was adjusted by adding HCl or NaOH aqueous solution.

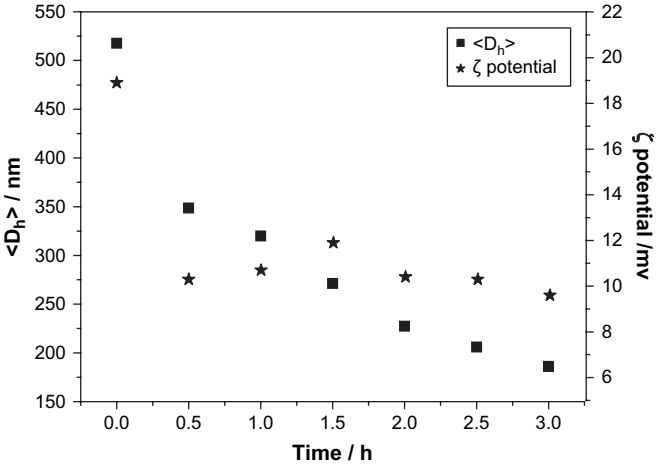

Fig. 1. Size and ζ potential of the reaction solution as a function of time (medium solution pH 3.0, ratio of AA/gelatin 2, concentration of gelatin 10 mg/mL).

size of the assemblies decreased in the pH range of 1.7–3.0. However, as for the cases of pH > 3.0 where the ζ potential decreased to below 10 mV, the repulsive force of the nanoparticles' surface possibly became too low to prevent secondary aggregations, thus resulting in a size increase. For simplicity, when adopting a gelatin concentration of 10 mg/mL and ratio of AA/gelatin of 2, NP-1.7 was used to denote the nanoparticles' solution obtained using medium solution of pH 1.7, NP-2.5 for using medium solution of pH 2.5, and so on.

Fig. 3 shows the sizes of nanoparticles' solutions prepared using medium solution of different pH value and those of NP-1.7 and NP-5.5 at different pH values obtained by adding NaOH or HCl solution. By comparing data points of curve A or C with curve B, we noticed that, at the same pH, the size of NP-1.7 was on the whole larger than that prepared using medium solution of different pH value while it was the opposite case for NP-5.5. This again suggests that the interactions in NP-5.5 are stronger than NP-1.7. Therefore, the

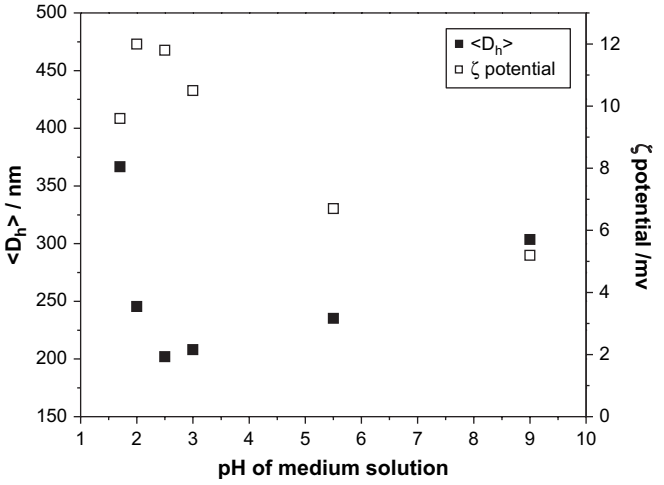

Fig. 2. $\langle D_h \rangle$ and ζ potential of nanoparticles' solution obtained by using medium solutions with different pH values (ratio of AA/gelatin 2, concentration of gelatin 10 mg/mL).

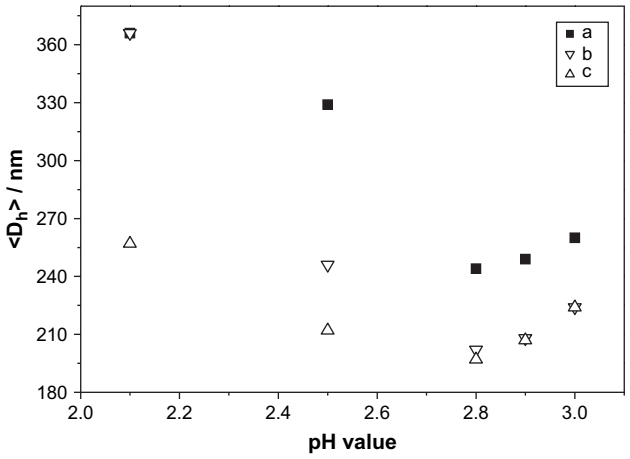

Fig. 3. $\langle D_h \rangle$ of nanoparticles' solutions as a function of pH value: (a) $\langle D_h \rangle$ of NP-1.7 at different pHs, (b) $\langle D_h \rangle$ of nanoparticles' solutions prepared using medium solution of different pHs, (c) $\langle D_h \rangle$ of NP-5.5 at different pHs.

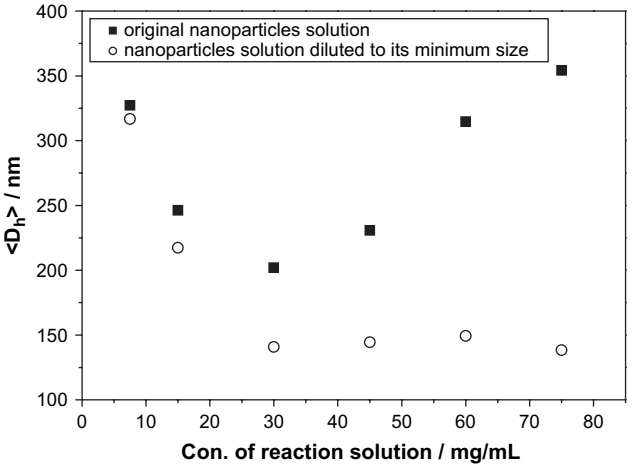

Fig. 4. Original sizes and minimum sizes (by dilution) of nanoparticles' solutions prepared at different concentrations (medium solution pH 2.5, ratio of AA/gelatin 2).

size and structure of nanoparticles can be controlled by changing pH of the medium solution.

3.1.2. Concentration effects

As disclosed in the previous papers [15], the typical simultaneous polymerization and self-assembly of template polymerization can slow down the self-assembly between the components, and hence can be used to prepare nanoparticles at high concentrations. And we wonder how high the concentration of the nanoparticles' solution can reach via template polymerization. Therefore, we made series of polymerizations at different concentrations. We found that when medium solution of pH 2.5 and AA/gelatin ratio of 2 were adopted, nanoparticles' solution of a concentration as high as 75 mg/mL can be prepared smoothly; however, when polymerization occurred at a higher concentration (90 mg/mL), besides the stable dispersed nanoparticles, some precipitants appeared at the later stage of the reaction. On the other hand, when polymerization was carried out at a concentration less than 7.5 mg/mL, the appearance of the reaction solution remained transparent throughout the process, indicating that no core-shell nanoparticles were formed. This was possibly because the molecular weight (3.2k) of PAA produced *in situ* under the condition did not reach the critical value, which is a requisite for the formation of insoluble gelatin–PAA complexes.

As revealed by DLS results illustrated in Fig. 4, we can see that, as the concentration of the reaction solution (preparation concentration) increased, the nanoparticles' size first decreased until reaching a minimum at a concentration of 30 mg/mL, and then increased continuously with the concentration.

As well known, the nanoparticles' size depends closely on its concentration due to the nanoparticles' aggregations. Therefore, the size of the original nanoparticles' solution may only reflect apparent size of the nanoparticles as the primary assemblies formed during the polymerization may aggregate due to concentration effect. Hence, we next examined the concentration–size dependence of the nanoparticles' solution by diluting with HCl solution of equal pH. It was found that the relations between the size and concentration of various nanoparticles' solutions were similar, and a typical curve of $\langle D_h \rangle$ vs. concentration for NP-2.5 is given in Fig. 5. Different from the monotonical decrease of the size with the concentration, which was often observed for nanoparticles [17], the size of NP-2.5 decreased with the concentration at a concentration above 0.6 mg/mL while it increased contrarily when further decreasing the concentration. It was easy to understand the size change in the range of 0.6–30 mg/mL. The size increase in the range of 0.15–0.3 mg/mL was possibly caused by the protonated gelatin shell, which may expand in dilute solution due to the electrostatic repulsion interactions.

Considering the concentration-dependence of the nanoparticles' size, we believe that the minimum size on $\langle D_h \rangle$–C curves of various nanoparticles was the real size of the primary assemblies formed in the reaction solution. As displayed in Fig. 4, the change of the minimum size with the preparation concentration is different from that of the original size. As

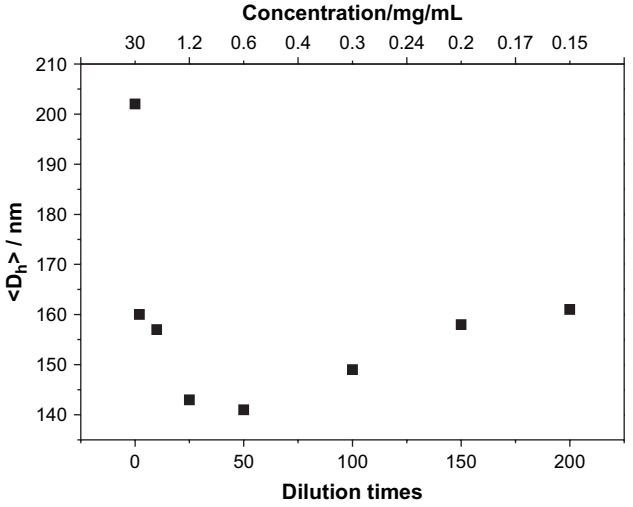

Fig. 5. Change of the size of NP-2.5 with dilution times.

the preparation concentration increased, the minimum size of nanoparticles' solution decreased substantially from 317 nm to 141 nm in a concentration range of 7.5–30 mg/mL while kept almost constant when the concentration was above 30 mg/mL. The initial decrease in the minimum size with the preparation concentration resulted from the enhancement in the interactions between the components, as the average molecular weight of PAA produced *in situ* increased with the concentration (Table 2). In addition, the difference between the original size of the nanoparticles' solution and its corresponding minimum size by dilution became larger as the preparation concentration increased, which again proved that the aggregation between the primary assemblies augmented with the concentration.

Table 3
$\langle D_h \rangle$, PDI, ζ potential and average molecular weight of PAA of various nanoparticles' solutions prepared at different ratios of AA/gelatin[a]

Ratio of AA/gelatin (wt.)	Nanoparticles' solution[b]			Average molecular weight of PAA
	$\langle D_h \rangle$ (nm)	PDI	ζ potential (mV)	
0.5[c]	–	–	–	3.5k
1.0	240	0.07	15.2	8.7k
2.0	141	0.07	19.9	10.4k
3.0	177	0.10	19.5	13.2k
4.0	196	0.10	18.6	15.6k
5.0	267	0.10	16.4	16.6k
6.0	336	0.17	13.4	17.5k

[a] Gelatin solution of 10 mg/mL and medium solution of pH 2.5 were adopted.
[b] Nanoparticles' solution was diluted to its minimum size.
[c] No nanoparticles were formed at the end of polymerization.

3.1.3. AA/gelatin ratio effects

As the composition also affects the interactions between the components, we investigated the polymerizations at different ratios of AA/gelatin while keeping the concentration (10 mg/mL) of gelatin constant. We found that nanoparticles with fairly narrow size distributions can be prepared in a ratio range of 1.0–5.0. Due to the low molecular weight of PAA produced *in situ* (Table 3), no nanoparticles were produced at a ratio of 0.5. From the molecular weight data of PAA listed in Table 2 and 3, the critical molecular weight required for PAA to form insoluble complex with gelatin is estimated to be around 3.8k. In addition, when polymerizing at a ratio of 6.0 or larger, some precipitants tended to be produced at the end of the polymerization. The precipitants probably resulted from the interactions between the excess PAA produced *in situ* and gelatin shell of the nanoparticles at the later stage of the polymerization as there was no free gelatin available for assembling with PAA.

The average hydrodynamic diameters, size distributions, and ζ potentials of a series of nanoparticles' solutions prepared by changing AA/gelatin ratio were assembled in Table 3, and three facts could be drawn as follows. First, as the AA/gelatin ratio increased from 1.0 to 2.0, the minimum size of the nanoparticles, i.e., the size of the primary assemblies formed during the reaction, decreased substantially from 240 nm to 141 nm. Upon further increasing the ratio, the size increased on the contrary. Second, the size distributions of the primary assemblies obtained at different ratios were fairly narrow, except for the case of ratio 6.0. Third, the change of ζ potential with the ratio almost followed the opposite way of the size. That is, the ζ potential increased from 15.2 mV to 19.9 mV when the ratio increased from 1.0 to 2.0; after that, it decreased with the ratio. In the case of ratio 1.0, the weak interactions between gelatin and low molecular weight PAA led to the formation of large nanoparticles of loose structure. As the ratio increased to 2.0, the interactions were enhanced by a growth in both the number and the length of PAA chains, hence complexes with impact structure formed, causing a decrease in the size and an increase in the ζ potential. However, as the ratio increased to 3 or more, the further increase of the amount and the molecular weight of PAA led to the formation of large complexes' cores containing more PAA chains and shells of gelatin chains with less charges and contracted conformations. As a result, the nanoparticles' size increased while ζ potential decreased with the ratio in the range 2.0–6.0.

TEM was a powerful tool for observing the internal structure of polymeric assemblies. The morphology of nanoparticles prepared at different AA/gelatin ratios was observed by TEM. As displayed in Fig. 6, the contrast between the nanoparticles and the background of Fig. 6a was the lowest among the three micrographs, proving that the nanoparticles prepared at a AA/gelatin ratio of 1.0 have a loose structure. Also, the nanoparticles prepared at ratios 2.0 and 3.0 retained their circular contours while those prepared at a ratio of 1.0 deformed obviously. This may result from the flexibility of gelatin shells of the nanoparticles prepared at a ratio of 1.0 due to their weak interactions with PAA. Furthermore, after a close observation of Fig. 6a and 6b, one could discern a weak contrast between the periphery and the inner portion of the particles, which reveals the core-shell structure of the nanoparticles.

In addition, TEM sizes of the three nanoparticles were smaller than their corresponding DLS sizes due to the shrinkage of nanoparticles during the sample preparation. Also, the size-uniformity of the particles in TEM micrograph was conspicuously poorer than that of DLS size as indicated by its small polydispersity index (Table 3). This is possibly caused

Table 2
Molecular weight of PAA of various nanoparticles' solution prepared at different concentrations[a]

Preparation concentration (mg/mL)	3.75[b]	7.50	15.0	30.0	45.0	60.0	75.0
Average molecular weight of PAA	3.2k	3.8k	7.1k	10.4k	14.5k	14.8k	19.4k

[a] Medium solution of pH 2.5 and ratio of AA/gelatin of 2.0 were adopted.
[b] No nanoparticles were formed at the end of polymerization.

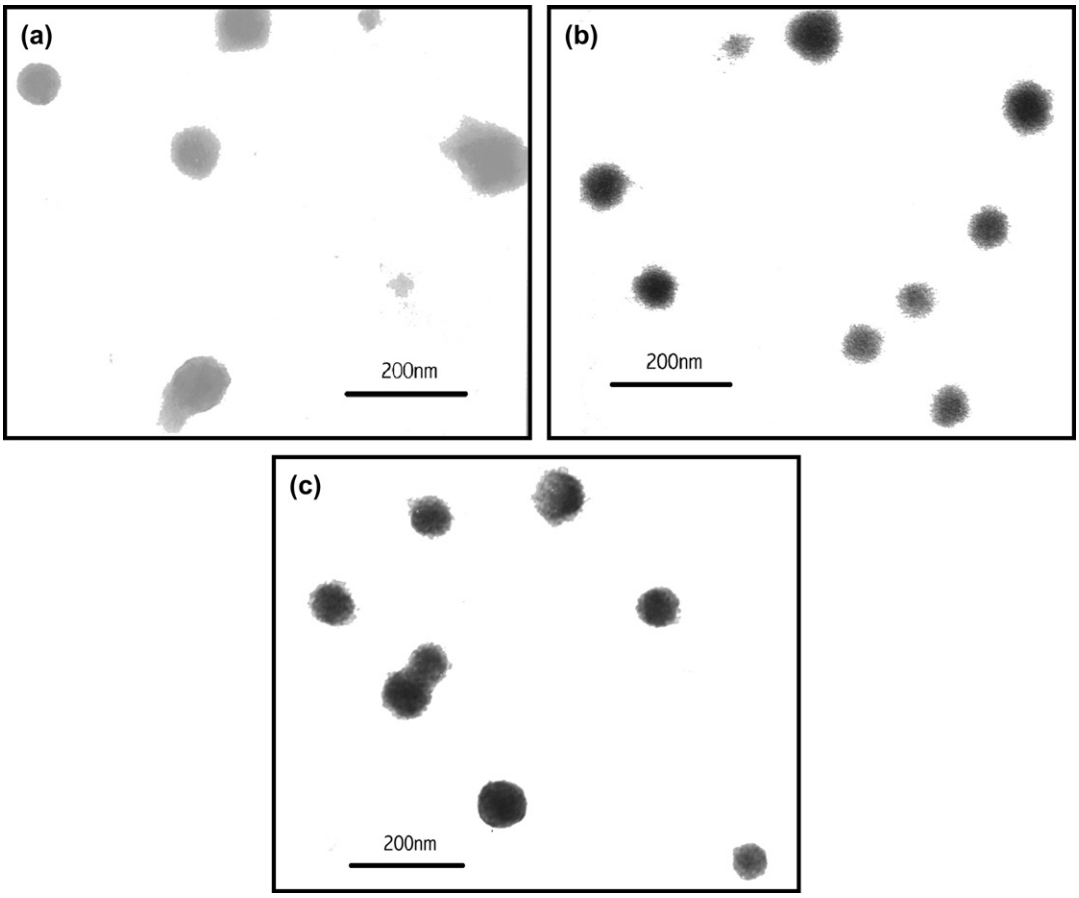

Fig. 6. TEM images of nanoparticles prepared at different AA/gelatin ratios: (a) 1.0, (b) 2.0, (c) 3.0.

by the difference in the shrinkage of the nanoparticles during drying due to the structural dissimilarity. As the nanoparticles result from the self-assembly between gelatin and PAA produced *in situ*, the nanoparticles produced at the early stage of the polymerization may bear small cores and large shells as there are lots of gelatin chains available for assembling with PAA chains. As the polymerization proceeds, the amount of gelatin chains available decreased gradually, which possibly results in nanoparticles with large cores and small shells at the later stage of the polymerization.

In order to compare the magnitude of the interactions among the series nanoparticles prepared by changing AA/gelatin ratio, we also studied their swelling capacity, which was defined as the ratio of DLS size of the nanoparticles' solution at pH 4.6 to that at pH 2.8, ($S_c = \langle D_h \rangle_{pH4.6} / \langle D_h \rangle_{pH2.8}$). The results are summarized in Table 4. Due to the interactions between PAA and gelatin, the IP of gelatin shell of the nanoparticles (around pH 4.0) was lower than that of pure gelatin (pH 4.8). As pH increases above 4.0, both the hydrogen bonding and electrostatic interactions between PAA and gelatin decrease with the increase of pH, as a result, the nanoparticles swell. The swelling capability of the nanoparticles decreased as the ratio of AA/gelatin increased, suggesting that the interactions in the nanoparticles increased with the ratio of AA/gelatin.

Table 4
Swelling capacity data of the series nanoparticles prepared at different AA/gelatin ratios[a]

Ratio of AA/gelatin (wt)	pH 2.8		pH 4.6[b]		S_c
	$\langle D_h \rangle$ (nm)	PDI	$\langle D_h \rangle$ (nm)	PDI	
1.0	244	0.09	650	0.31	2.7
2.0	157	0.04	362	0.17	2.3
3.0	211	0.07	403	0.17	1.9
4.0	230	0.15	389	0.15	1.7
5.0	251	0.12	379	0.14	1.5

[a] Nanoparticles' solution was diluted to 1/10 concentration before adjusting pH value to 2.8 and 4.6 by adding NaOH solution.
[b] The nanoparticles retained their structure integrity at pH 4.6 (see Section 3.3).

3.2. FTIR analysis of PAA/gelatin nanoparticles

To illustrate the interactions in PAA/gelatin nanoparticles, we measured FTIR spectra of the nanoparticles and their component polymers, the results are presented in Fig. 7. For pure PAA, the stretching vibrations of −OH and carboxy carbonyl appeared around 3431 cm^{-1} and 1710 cm^{-1}, respectively. For pure gelatin, the stretching vibrations of −NH− and amide carbonyl appeared around 3417 cm^{-1} and 1647 cm^{-1}, respectively. On the spectrum of PAA/gelatin nanoparticles (pH 2.8),

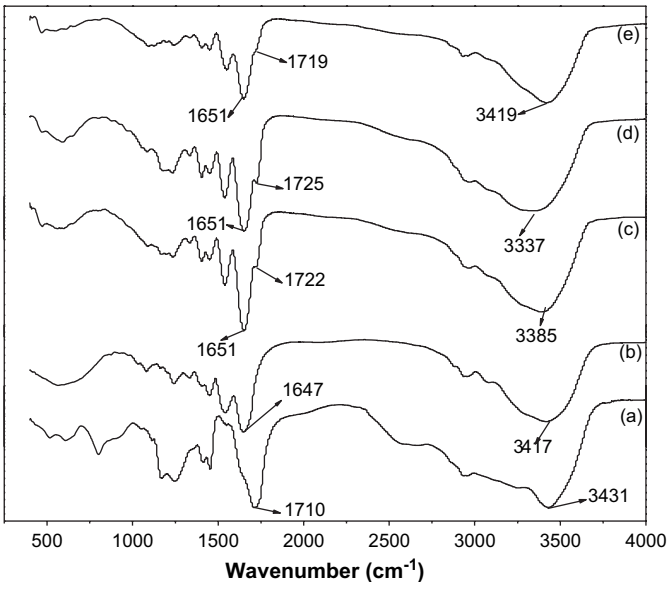

Fig. 7. FTIR spectra of PAA/gelatin nanoparticles and the components: (a) PAA, (b) gelatin, (c) NP-2.5 (pH 2.8), (d) NP-2.5 at pH 2.1 obtained by adding HCl solution to (c), (e) NP-2.5 at pH 4.6 obtained by adding NaOH solution to (c).

the stretching vibration bands of −NH− and −OH both shifted to a lower wave number and merged into one band around 3385 cm^{-1}; meanwhile, the stretching vibration bands of amido carbonyl and carboxyl carbonyl both shifted to a higher wave number and moved to 1651 cm^{-1} and 1722 cm^{-1}, respectively. This demonstrated hydrogen bonding interactions between amido of gelatin and carboxyl of PAA [18,19]. By comparing curves c−e of Fig. 7, one can see that, as pH increased from 2.1 to 4.8, −OH band shifted progressively from 3337 cm^{-1} to 3419 cm^{-1} and carboxyl carbonyl band from 1725 cm^{-1} to 1719 cm^{-1}; meanwhile, the area of carboxyl carbonyl band became smaller, suggesting that hydrogen bonding interactions of the nanoparticles decreased with the increasing of pH value.

3.3. pH-responsive behavior of PAA/gelatin nanoparticles

The structure and size of PAA/gelatin nanoparticles not only depended on pH of the medium solution adopted, but also on pH of the nanoparticles' solution. We studied the pH-response of the nanoparticles' structure and size of NP-2.5 in a pH range of 1.0−6.0. As shown in Fig. 8, the change in the hydrodynamic diameter of the nanoparticles with pH was found complicated: as pH increased, the size decreased in pH ranges of 1.2−2.8 and 4.6−5.6 while increased in pH range of 2.8−3.5. Meanwhile, the ζ potential exhibited an initial increase in pH range of 1.2−2.8 and a subsequent decrease in pH range of 2.8−5.6. Key determinants in pH-induced change of the nanoparticles' size are the ionization of the components in the medium. As pH decreased from 2.8 to 1.2, the ionization of PAA decreased, leading to a replacement of strong electrostatic interactions between $-COO^-$ and $-NH_3^+$ by weak hydrogen bonds between −COOH and −CONH−,

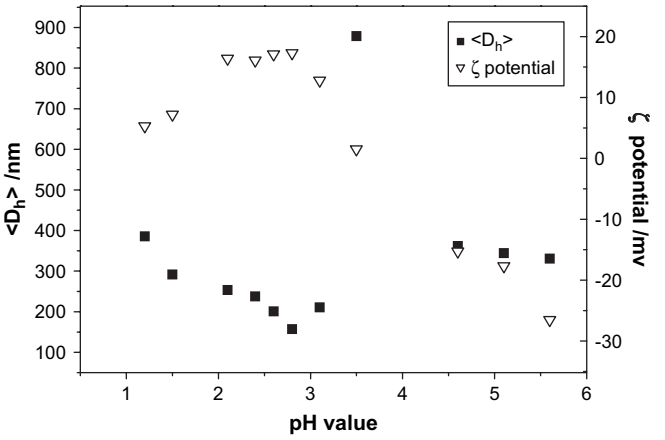

Fig. 8. Size and ζ potential of NP-2.5 solution (3 mg/mL) at different pH values, pH of the solution was adjusted by adding NaOH or HCl aqueous solution to the starting solution of pH 2.8 and concentration 3 mg/mL.

and subsequently a volume expansion of the nanoparticles. The change of ζ potential of the nanoparticles with pH in pH range of 1.2−2.8 is similar to that of gelatin, and its substantial decrease in pH 1.5−1.2 may result from the charge-shielding effects of ions introduced during pH adjustment. In the second zone (pH 2.8−3.5), the size increase with the pH may result from the nanoparticles' aggregations due to their fairly low ζ potentials. And as ζ potential was close to zero, the aggregations led to a rapid size increase. In the third zone (pH 4.6−5.6), the nanoparticles remained stable at pH 4.6 ($\langle D_h \rangle = 362$ nm, PDI = 0.14) although its ζ potential was quite negative (−15 mV), indicating the balance between the hydrophobic and hydrophilic interactions in the nanoparticles made them swell while still retaining their whole structures. Upon further increasing pH, the further enhancement in the repulsive interactions would lead to the disintegration of the nanoparticles' structure and subsequently a size decrease. In addition, on the hydrodynamic diameter distribution curve of the nanoparticles at pH 5.6, besides the main peak, there appeared a second small peak around 30 nm, which may correspond to fragments dropped from the nanoparticles.

Pyrene has commonly been used as a hydrophobic fluorescence probe to evaluate the polarity of various microenvironments [20]. Changes in the relative intensity of the first and third vibration bands (ratio of I_1/I_3) in the pyrene emission spectrum have proven to be reliable tools in examining the polarity of the microenvironment [21,22]. Here, we use pyrene as the fluorescence probe to investigate the hydrophobicity/hydrophilicity of PAA/gelatin nanoparticles. Fig. 9 displays the change in ratio of I_1/I_3 of NP-2.5 with the pH value. In a pH range of 1.2−5.6, the ratio of I_1/I_3 of NP-2.5 was the lowest at pH 1.2, where hydrogen bonding interactions dominated in the nanoparticles. As pH increased, the ratio of I_1/I_3 increased slowly with the pH value except for pH 3.5, indicating that the nanoparticles became more hydrophilic as H-bond interactions were replaced by electrostatic interactions. For the case of pH 3.5 where the ζ potential was close to zero, the nanoparticles aggregated badly, causing lots of nanoparticles' precipitate at the bottom of the cell during fluorescence tests.

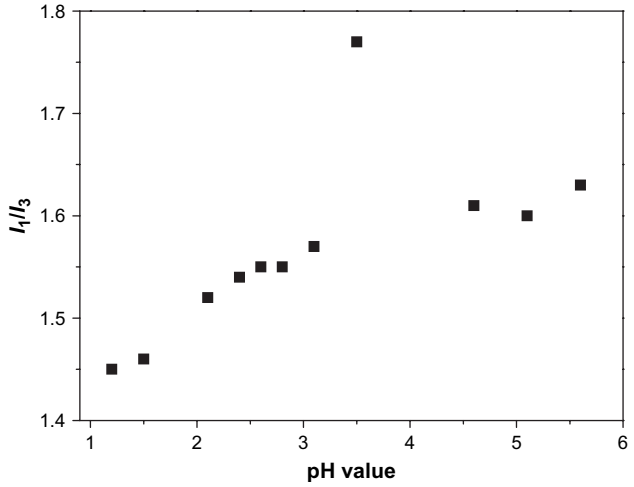

Fig. 9. Ratio of I_1/I_3 of pyrene/NP-2.5 solution (3 mg/mL) at different pH values.

As a result, the ratio of I_1/I_3 was large and close to that of pure water (1.9).

3.4. Salt-response of PAA/gelatin nanoparticles

Due to the shielding effect of ions on the charge, pH-responsive nanoparticles always also exhibit salt-sensitivity at a certain degree. We studied the salt-dependence of the nanoparticles' size. In fact, the nanoparticles' size was found to vary with salt (NaCl) concentration, and the trend of change in nanoparticles' size shows two opposite ways with the salt concentration (Fig. 10). As the salt concentration increased, the size decreased slowly until reaching a minimum (145 nm) at a salt concentration of 0.04 mol/L; after that, it increased on the contrary. The salt-dependence of the nanoparticles' size in the range of 0–0.04 mol/L agreed with that of negatively charged crosslinked PAA hollow spheres reported by Jiang [23] while the salt-dependence in the range of 0.04–0.35 mol/L corresponded to that of positively charged hollow spheres reported by Jiang [13b]. Both the above two opposite changes could be attributed to the screening of the salt on the surface charge of the nanoparticles. In the low salt concentration zone, the introduction of the salt would cause a decrease in the surface charge and thus a contraction in the nanoparticles' shell. Meanwhile, the surface charge of the nanoparticles, although decreased, remained high enough to keep the nanoparticles from secondary aggregations. However, in the high salt concentration zone, further decrease in the surface charge made it fail to exclude aggregations between the nanoparticles. And the aggregations increased with the salt concentration. As a result, the nanoparticles' size increased slowly. As indicated by ζ potential data illustrated in Fig. 10, the aggregations began to occur when ζ potential was below 12 mV. We also found that when ζ potential decreased to around zero, the aggregations led to a drastic increase in the nanoparticles' size (data not shown).

PAA/gelatin nanoparticles could also be prepared by dropping method but at a lower concentration. To compare salt-dependences between the nanoparticles prepared by the two methods, we also prepared nanoparticles via dropping method at a similar pH, that is, dropping equal volume of PAA solution (4 mg/mL, pH 2.8) dropwise into gelatin solution (2 mg/mL, pH 2.8). Different from the parabola-like size change of NP-2.5 (Fig. 10), the size of the nanoparticles prepared by dropping method increased monotonically with the salt concentration (Fig. 11), which was due to its lower ζ potential (4.3 mV) as compared with that of NP-2.5 (17.4 mV). In the case of the nanoparticles prepared by dropping method, many gelatin chains were wrapped into nanoparticles' cores due to their fairly fast assembling process. As a result, nanoparticles with a larger size and a smaller surface charge were formed. Obviously, nanoparticles prepared via template polymerization have a higher salt-resistance.

3.5. Crosslinking of PAA/gelatin nanoparticles with glutaraldehyde

As disclosed above, PAA/gelatin nanoparticles tend to disintegrate when pH > 4.6 due to the decomplexation between

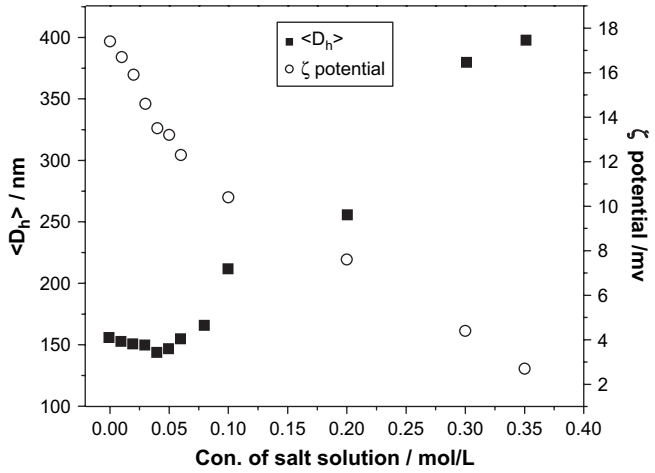

Fig. 10. ζ potential and size of NP-2.5 (3 mg/mL) at different salt concentrations.

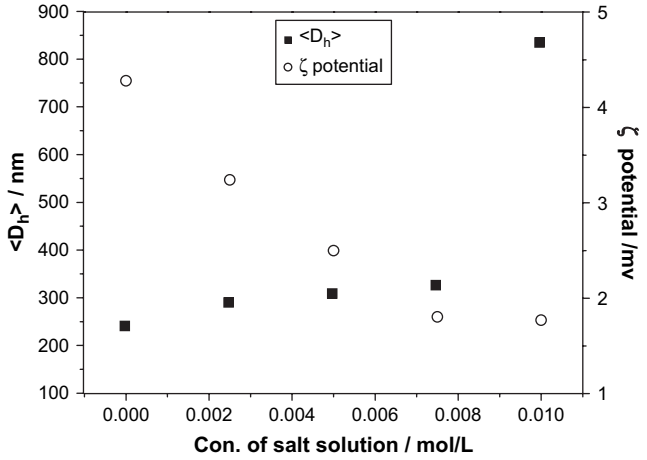

Fig. 11. ζ potential and size of nanoparticles prepared by dropping method at different salt concentrations.

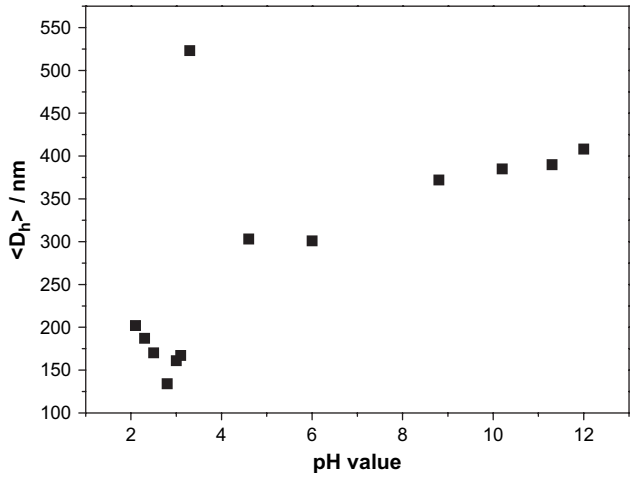

Fig. 12. Size and ζ potential of crosslinked PAA/gelatin nanoparticles obtained from NP-2.5 solution of concentration 3 mg/mL at a GA/gelatin ratio of 10%.

the components. To improve their stability in neutral and basic media, GA was used to selectively crosslink gelatin to lock the nanoparticles' structure. It is well known that nucleophilic reaction between amino groups and aldehyde groups produces Schiff's base, which is also the main product of the reaction between GA and gelatin. After crosslinking at 40 °C for 2 h at a weight ratio of GA/gelatin of 10%, the size of the nanoparticles shrank slightly from 157 nm to 134 nm, which was caused by the constriction of gelatin network formed by crosslinking. The success of locking-in the nanoparticles' structure via crosslinking was confirmed by the stable existence of crosslinked nanoparticles in basic media as displayed in Fig. 12. As compared with Fig. 8, curves of size vs. pH of the nanoparticles before and after crosslinkig in pH range of 2.0–4.6 were similar, except that the size of crosslinked ones was smaller. In addition, even after pH reached above 4.6, the crosslinked nanoparticles remained stable in the solution and their size increased monotonically with pH due to the decomplexation between PAA and gelatin and the repulsion interactions among $-COO^-$ of PAA and gelatin.

Table 5
Size data of crosslinked[a] NP-2.5 at different ratios of GA/gelatin

GA/gelatin (%)	pH 2.8		pH 6.0		S_c
	$\langle D_h \rangle$ (nm)	PDI	$\langle D_h \rangle$ (nm)	PDI	$(\langle D_h \rangle_{pH6.0}/\langle D_h \rangle_{pH2.8})$
0	157	0.09	–	–	–
5	144	0.05	420	0.51[b]	2.92
10	134	0.04	301	0.14	2.25
15	132	0.05	264	0.13	2.00
20	129	0.02	249	0.12	1.93
30	131	0.02	244	0.06	1.86
40	138	0.06	239	0.08	1.73

[a] Crosslinking was undertaken in diluted nanoparticles' solutions (3 mg/mL).
[b] Double peaks appeared in the D_h distribution curve.

Fig. 13 presents AFM images of NP-2.5 before and after crosslinking. Before crosslinking, the nanoparticles' diameter ranged from 133 to 332 nm with an average value of about 240 nm. Meanwhile, the average height of the nanoparticles was only about 19 nm (Fig. 13a). This demonstrated that the nanoparticles badly collapsed on the mica substrate. Upon crosslinking, the average diameter of the nanoparticles decreased dramatically to about 181 nm and the diameter range (156–213 nm) became narrow while their average height increased substantially to about 30 nm. This revealed that the nanoparticles became stiff after crosslinking.

It is obvious that the swelling capacity of crosslinked nanoparticles depends on their crosslinking degree. We examined the swelling ratio (S_c, i.e. $\langle D_h \rangle_{pH6.0}/\langle D_h \rangle_{pH2.8}$) of various crosslinked nanoparticles prepared at different ratios of GA/gelatin, the results are assembled in Table 5. Several facts could be drawn from Table 5 as follows. First, as GA/gelatin ratio increased from 0% to 20%, the nanoparticles' size decreased slowly with the ratio while it increased slightly as the ratio was further increased to 40%. This was because at a high ratio of GA/gelatin, besides the intra-nanoparticles' crosslinking, some inter-nanoparticles' crosslinking may also occur. Secondly, in a GA/gelatin ratio range of 10–30%, the nanoparticles' structure was perfectly locked by crosslinking. However, a ratio of 5% failed to lock the nanoparticles'

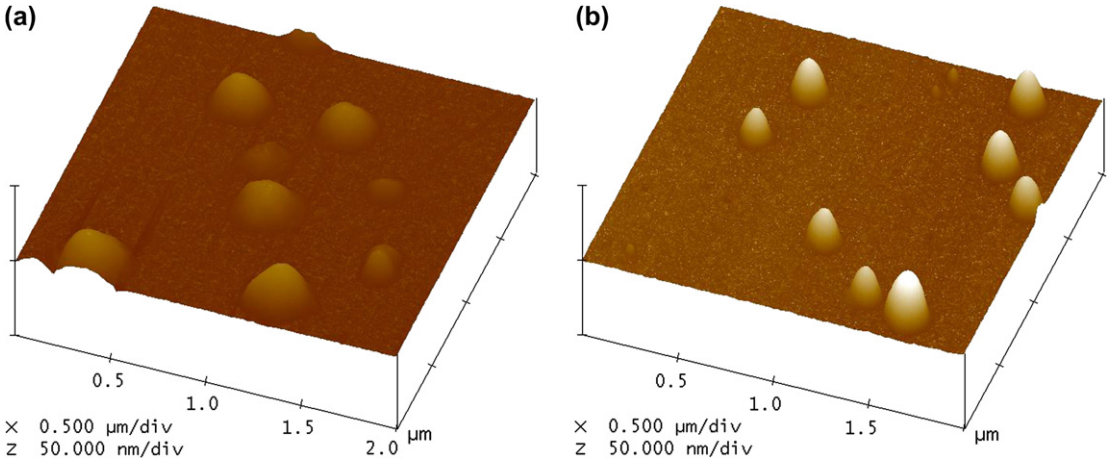

Fig. 13. AFM images of NP-2.5 before (a) and after (b) crosslinking.

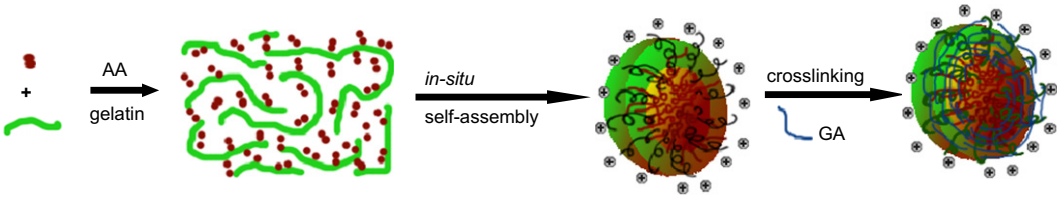

Scheme 1. Schematic illustration of preparing PAA/gelatin nanoparticles via template polymerization.

structure as indicated by its DLS data at pH 6.0: besides the main peak around 430 nm, a second small peak around 56 nm was also observed on its distribution curve. Finally, the swelling capacity of the nanoparticles decreased with the increasing of the ratio. It was understandable as the resistance against swelling of the nanoparticles increased with the crosslinking degree. In addition, the above selective crosslinking could also be carried out in original NP-2.5 solution (30 mg/mL). For example, after crosslinking at a GA/gelatin ratio of 10%, the nanoparticles' size changed from the initial 202 nm to 175 nm (pH = 2.8). And the size swelled to 298 nm when pH of the solution was further adjusted to pH 6.0.

4. Conclusion

Taking advantage of the simultaneous polymerization and self-assembly between the components in the template polymerization, PAA/gelatin core-shell nanoparticles could be synthesized at a concentration as high as 75 mg/mL. The nanoparticles' structure was further locked by selective crosslinking gelatin with GA (Scheme 1). The size and structure of the nanoparticles can be adjusted by varying polymerization parameters. Nanoparticles with a smaller size and more compact structure could be obtained by increasing the pH of the medium solution. As the reaction concentration or ratio of AA/gelatin increased, there was an initial decrease and subsequent increase in the nanoparticles' size; meanwhile, the nanoparticles' structure became more compact.

The hydrogen bonding interactions in the nanoparticles and their decrease with increasing pH value were confirmed by FTIR. The obtained PAA/gelatin nanoparticles are responsive to pH and salt. The salt-dependence of the nanoparticles' size was parabolic with a minimum size at a salt concentration of 0.04 mol/L. Furthermore, the nanoparticles can resist against a salt concentration higher than those prepared by dropping method. Finally, the crosslinked nanoparticles remained stable in basic media and swelled substantially as the medium changed from acid to base. And the swelling capacity decreased with the increase of crosslinking degree.

Acknowledgements

This work was supported by the National Natural Science Foundation of China (NNSFC No.20604006) and Director Foundation of State Key Laboratory for Modification of Chemical Fibers and Polymer Materials. The authors also thank Prof. Meifang Zhu of Donghua University for her kindly help.

References

[1] Stolnik S, Illum L, Davis SS. Adv Drug Deliv Rev 1995;16(2–3):195–214.
[2] Dresco PA, Zaitsev VS, Gambino RJ, Chu B. Langmuir 1999;15(6):1945–51.
[3] Tungittiplakorn W, Lion LW, Cohen C, Kim JY. Environ Sci Technol 2004;38(5):1605–10.
[4] Zawaneh PN, Doody AM, Zelikin AN, Putnam D. Biomacromolecules 2006;7(11):3245–51.
[5] Tian L, Hammond PT. Chem Mater 2006;18(17):3976–84.
[6] Moghimi SM, Hunter AC, Murray JC. Pharmacol Rev 2001;53(2):283–318.
[7] Gref R, Luck M, Quellec P, Marchand M, Dellacherie E, Harnisch S, et al. Colloids Surf B 2000;18(3–4):301–13.
[8] Zambaux MF, Bonneaux F, Gref R, Dellacherie E, Vigneron C. J Biomed Mater Res 1999;44(1):109–15.
[9] Zhang Q, Remsen EE, Wooley KL. J Am Chem Soc 2000;122(15):3642–51.
[10] Bütün V, Billingham NC, Armes SP. J Am Chem Soc 1998;120(45):11818–9;
Liu SY, Armes SP. J Am Chem Soc 2001;123(40):9910–1.
[11] Chen DY, Peng HS, Jiang M. Macromolecules 2003;36(8):2576–8.
[12] Chen Q, Hu Y, Chen Y, Jiang XQ, Yang YG. Macromol Biosci 2005;5(10):993–1000.
[13] (a) Hu Y, Jiang XQ, Ding Y, Ge HX, Yuan Y. Biomaterials 2002;23(15):3193–201;
(b) Hu Y, Chen Y, Chen Q, Zhang LY, Jiang XQ, Yang CZ. Polymer 2004;46(26):12703–10.
[14] Tang MH, Dou HJ, Sun K. Polymer 2006;47(2):728–34.
[15] Wang ZX, Zhang YW, Wang YS, Zhao JX, Wu CX. J Macromol Sci Part A 2006;43:1779–86;
Zhang YW, Wang ZX, Wang YS, Zhao JX, Wu CX. Polymer 2007;48(19):5639–45.
[16] Ahn JS, Choi HK, Cho CS. Biomaterials 2001;22(9):923–8.
[17] Yu YS, Eisenberg A. J Am Chem Soc 1997;119(35):8383–4.
[18] Gonzalez-Blanco C, Rodriguez LJ, Velasquez MM. Langmuir 1997;13(7):1938–45.
[19] Chamekh OM, Nguyen QT, Metayer M, Saiter M, Garda MR. Polymer 2004;45(7):4181–7.
[20] Szajdzinska-Pietek E, Wolszczak M, Plonka A, Schlick S. J Am Chem Soc 1998;120(17):4215–21.
[21] Hierrezuelo JM, Aguiar J, Ruiz CC. Langmuir 2004;20(24):10419–26.
[22] Siu H, Duhamel J. J Phys Chem B 2005;109(5):1770–80.
[23] Zhang YW, Jiang M, Zhao JX, Wang ZX, Dou HJ, Chen DY. Langmuir 2005;21(4):1531–8.